Biochemical and Biophysical Research Communications 556 (2021) 45–52

Contents lists available at ScienceDirect

Biochemical and Biophysical Research Communications

journal homepage: www.elsevier.com/locate/ybbrc

The miRISC component AGO2 has multiple binding sites for Nup358 SUMO-interacting motif

Prachi Deshmukh [a], Shubha Markande [a], Vikas Fandade [a], Yogendra Ramtirtha [b], Mallur Srivatsan Madhusudhan [b], Jomon Joseph [a, *]

[a] National Centre for Cell Science, S.P. Pune University Campus, Pune, India
[b] Division of Biology, Indian Institute of Science Education and Research, Pune, India

ARTICLE INFO

Article history:
Received 19 March 2021
Accepted 25 March 2021
Available online 7 April 2021

Keywords:
miRNA
Nup358
SUMO-interaction motif
AGO2
Dicer
Hsp90

ABSTRACT

Micro-RNA mediated suppression of mRNA translation represents a major regulatory mode of post-transcriptional gene expression. Recently, the nucleoporin Nup358 was shown to interact with AGO protein, a key component of miRNA-induced silencing complex (miRISC), and facilitate the coupling of miRISC with target mRNA. Previous results suggested that SUMO-interacting motifs (SIMs) present on Nup358 mediate interaction with AGO protein. Here we show that Nup358-SIM has multiple interacting regions on AGO2, specifically within the N, PAZ and MID domains, with an affinity comparable to SIM-SUMO1 interaction. The study also unraveled specific residues involved in the interaction of AGO2 with miRNA-loading components such as Dicer and HSP90. Collectively, the results support the conclusion that multiple SIMs contribute to the association of Nup358 with AGO2.

1. Introduction

MicroRNAs (miRNAs) are a class of short single-stranded non-coding RNAs of around 20–22 nucleotide length [1]. Small RNA (miRNA) loaded Argonaute (AGO) protein forms the core of miRNA Induced Silencing Complex (miRISC), which binds to the complementary region of target mRNA and leads to either degradation or suppression of the mRNA [2,3]. Once transcribed and processed by the microprocessor complex in the nucleus, the stem-loop containing precursor miRNA (pre-miRNA) is exported from the nucleus into the cytoplasm [4]. Then the endonuclease Dicer, along with TRBP, removes the loop structure to produce mature double-stranded miRNA, which with the help of HSP90 is loaded onto AGO proteins [3]. The miRNA-loaded AGO protein (miRISC), binds to specific target mRNA based on the sequence complementarity between mRNA and miRNA and with the aid of GW182 (TNRC6) protein silences the expression of the encoding gene [5].

AGO has four functional domains; N-terminal (N), Piwi–Argonaute–Zwille (PAZ), middle (MID), P-element Induced WImpy testis (PIWI) and two linker domains L1 and L2 [3]. Electron microscopic studies and EM reconstructions suggested that PIWI and MID domains of AGO2 interact with the platform structure of Dicer, whereas AGO2 N-terminal domain interacts with Dicer's base branch giving rise to a triangular architecture for the complex [6]. The AGO2 PIWI domain specifically interacts with the Dicer RNaseIIIa domain [7]. HSP90 is shown to interact with the N domain of AGO and mediate the loading of miRNA onto AGO proteins [8].

It is still unclear how a given miRISC finds its target mRNA among the large pool of mRNAs in the cytoplasmic milieu. Studies from our laboratory uncovered a role for the nucleoporin Nup358 in promoting the coupling of miRISC with its target mRNA in mammalian cells [9]. This potentially involves the cytoplasmically located Nup358 on the ER as a part of annulate lamellae [9]. It was also shown that Nup358 directly interacts with AGO proteins through its SUMO-interacting motifs (SIMs). Interestingly, SIM also binds to other AGO clade proteins, indicating SIM to be a general AGO-interacting motif [9]. SIM represents a beta-sheet comprising of 8–10 amino acids and is a well-characterized SUMO-binding motif [10]. Interestingly, mutation of the critical hydrophobic residues in SIM involved in the interaction with SUMO also abolished binding with AGO2, indicating similarity in the molecular nature of the interaction between SIM-SUMO and SIM-AGO2 [9].

Here we further characterized the SIM-binding sites on AGO2 protein. The results showed that N, PAZ and MID domains independently can bind to Nup358-SIM with an affinity range similar to

* Corresponding author. National Centre for Cell Science, S.P. Pune University Campus, Pune, 411007, Maharashtra State, India.
E-mail address: josephj@nccs.res.in (J. Joseph).

https://doi.org/10.1016/j.bbrc.2021.03.140
0006-291X/

that of SIM-SUMO interaction. During this study, we also identified specific residues that contribute to the binding of AGO2 with Dicer and HSP90 proteins.

2. Materials and methods

2.1. Cell culture and transfection

HEK293T cells were grown in Dulbecco's modified Eagle's medium (Invitrogen) with 10% heat-inactivated fetal bovine serum (v/v) (Invitrogen) and 10 μg/ml ciprofloxacin antibiotics in a humidified incubator at 37 °C in 5% CO_2. For immunoprecipitation and western analyses, HEK293T cells were grown in 100 mm petriplates (1×10^7 cells per plate) or six-well plates (3×10^5 cells per well). After 12 h, cells were transfected with different plasmids using polyethyleneimine linear (PEI, MW-25000 kDa, Polysciences Corporation Ltd.), following the manufacturer's instructions.

2.2. Plasmids

pcDNA-HA-hAGO2 (HA-AGO2) construct was described earlier [9]. For expression of different domains of human AGO2, regions corresponding to 1–229 (AGO2-N), 230–445 (AGO2-PAZ), 446–580 (AGO2-MID), 581–859 amino acids (AGO2-PIWI) using pcDNA-HA-AGO2 were cloned at EcoRI/SmaI sites of modified pCIneo-NHA vector (a kind gift from Ramesh Pillai, University of Geneva, Switzerland). The MBP tagged AGO2 domains (N, PAZ, MID and PIWI) were generated by subcloning the corresponding regions from pCIneo-NHA constructs into pMAL c2 vector (New England BioLabs) at EcoRI/HindIII sites. Human AGO2 fragments - AGO2-N1 (1–66 aa), AGO2-N2 (67–138 aa), AGO2-N3 (139–229 aa) were generated using pMAL-c2 vector. For bacterial expression of His-IR1, human Nup358 (2631–2708 aa) was cloned into pET30 vector (Novagen).

For the generation of deletion mutants of AGO2, specific primers were used to amplify regions corresponding to 230–859 aa (hAGO2ΔN), 1–580 aa (hAGO2ΔPIWI) using pcDNA-HA-AGO2 as a template and cloned into pcDNA-HA vector. To generate hAGO2Δ PAZ (Δ230–445 aa) and hAGO2ΔMID (Δ446–580 aa) mutants, appropriate primers were used to PCR-amplify the entire pcDNA-HA-AGO2 construct, devoid of the corresponding regions, and the products were self-ligated. Point mutations in AGO2 (hAGO2-L115A/V117A, hAGO2-F491A/Y494A, hAGO2-V629A/V631A, hAGO2-F491A/K493A, hAGO2-L508A/Y512A) were introduced by a PCR-based method using mutant primers. All constructs were verified by sequencing.

2.3. Immunoprecipitation and western blotting

Co-immunoprecipitation (co-IP) of GFP-SIM with AGO2 wild type and mutants was performed as described earlier [9]. Briefly, HEK293T cells expressing indicated constructs were lysed in a buffer (20 mM Tris–HCl, pH 8.0, 137 mM NaCl, 10% Glycerol, 0.5% NP-40, 2 mM EDTA) supplemented with 7.5 mM sodium fluoride, 0.75 mM sodium orthovanadate, 1 mM PMSF, protease inhibitor cocktail (Roche), leupeptin 50 μg/ml, aprotinin 5 μg/ml, and pepstatin 2 μg/ml. Immunoprecipitation was performed by incubating the precleared lysate with EZview™ Red Anti-HA Affinity beads (Sigma) for 2 h at 4 °C on rotospin (Bangalore Genei). The immunoprecipitates were separated by SDS–PAGE and transferred to PVDF membrane (Millipore) using semi-dry transfer apparatus (GE Healthcare). The PVDF membranes were then incubated with the primary antibody in 1% BSA in TBS with 0.1% Tween-20 (TBST) for 2 h at RT or overnight at 4 °C. Membranes were washed thrice with TBST for 3 min each and incubated with HRP-conjugated secondary antibodies (GE Healthcare) in 1% BSA in TBST for 1 h. Further, the membranes were washed and developed using ECL Plus Western Detection Kit (GE Healthcare or Thermo Scientific) following the manufacturer's instructions. The images were acquired using ImageQuant LAS 4000 (GE Healthcare).

The following antibodies and dilutions were used for western blotting: rabbit anti-Dicer (1:1,500; CST, 53625), mouse anti-GFP (1:8,000; Santa Cruz Biotechnology Inc., sc-9996), mouse anti-HA (1:5,000; Covance Research Products, MMS-101R), mouse anti-HSP90 (1:6000; R&D systems, MAB3286), Sheep anti-rabbit IgG-HRP (1:10,000; GE Healthcare, NA-934), sheep anti-mouse IgG-HRP (1:10,000; GE Healthcare, NA-931).

2.4. Bacterial expression and in vitro pull-down assays

For the purification of His-IR1 protein, the plasmid pET30-IR1 was transformed into *Escherichia coli* BL21 DE3 RIL strain and induced with 0.5 mM IPTG at 18 °C for 6 h. Cells were lysed in lysis buffer (50 mM Tris (pH 8.0), 300 mM NaCl, 0.1% NP40, 5% glycerol) supplemented 1 mM PMSF, protease inhibitor cocktail (PIC, Roche) and lysozyme (200 μg/ml). Lysate was centrifuged at ~10,600 *g* for 30 min at 4 °C. The supernatant was incubated with Ni-NTA beads (Qiagen) for 2 h at 4 °C. The beads were then washed thrice with cold lysis buffer supplemented with 10 mM of Imidazole. His-IR1 protein was then eluted in elution buffer (50 mM Tris-HCl, pH 8.0, containing 300 mM NaCl, 0.1% NP40, 5% glycerol and 300 mM Imidazole). The protein was then dialyzed in PBS (10 mM Na_2HPO_4, 1.8 mM KH_2PO_4, pH 7.4, containing 137 mM NaCl and 2.7 mM KCl).

For purification of MBP-tagged proteins expressed in bacterial cells, corresponding constructs were transformed in *Escherichia coli* BL21 DE3 RIL strain and induced with 0.5 mM IPTG at 18 °C for 6 h. Cells were lysed in lysis buffer [50 mM Tris, pH 8.0 with 300 mM NaCl, 0.1% NP40, 5% glycerol and supplemented 1 mM PMSF, protease inhibitor cocktail (PIC, Roche), 1 mM DTT and 1 mM EDTA and lysozyme (200 μg/ml)]. Lysate was centrifuged at ~10,600 *g* for 30 min at 4 °C. The supernatant was then incubated with equilibrated amylose beads (New England BioLabs) for 1 h, washed with lysis buffer before eluting the protein in elution buffer (50 mM Tris-HCl, pH 8.0, 300 mM NaCl, 10 mM maltose, 0.5% Glycerol, 1 mM EDTA) followed by dialysis in a buffer (50 mM Tris-HCl, pH 8.0, 300 mM NaCl, 0.05% Tween, 50 μM EDTA). Size exclusion chromatography (SEC) was performed using Superdex 200 (16/600) to obtain the protein in monomeric form, which was used for further experiments. To perform the MBP pull-down assay, purified MBP-tagged proteins bound to amylose beads were incubated with an equal amount of His-IR1 protein for 1 h. After washing with the lysis buffer, the proteins were eluted in 3 × SDS-PAGE loading dye and subjected to SDS-PAGE analysis.

2.5. Surface plasmon resonance measurements

The kinetics of binding of AGO2 domains with SIM1 peptide was measured by single-cycle kinetics (SCK) using SPR-based biosensor Biacore T200 (Biacore, Uppsala, Sweden). Biotinylated SIM peptide (DNEIEVIIVWEKK) [11] was immobilized on the Sensor Chip CAP using Biotin CAPture Kit (28920233, GE Healthcare). All of the binding measurements were performed in running buffer (50 mM Tris-HCl, pH 8.0, 300 mM NaCl, 0.05% Tween, 50 μM EDTA and 1 mM DTT) at 25 °C. First, the conditioning of the chip was performed, and the Biotin CAPture reagent was flown through the flow cells 1 and 2. Next, the biotin-SIM1 peptide was immobilized on a flow cell 2 (FC2) of a sensor SA CAP chip whereas the first flow cell (FC1) was left blank and served as a control. To measure binding to SIM1 peptide, increasing concentrations (50, 100, 200, 400 and 800 μM) of the analytes (MBP-tagged proteins) were injected for

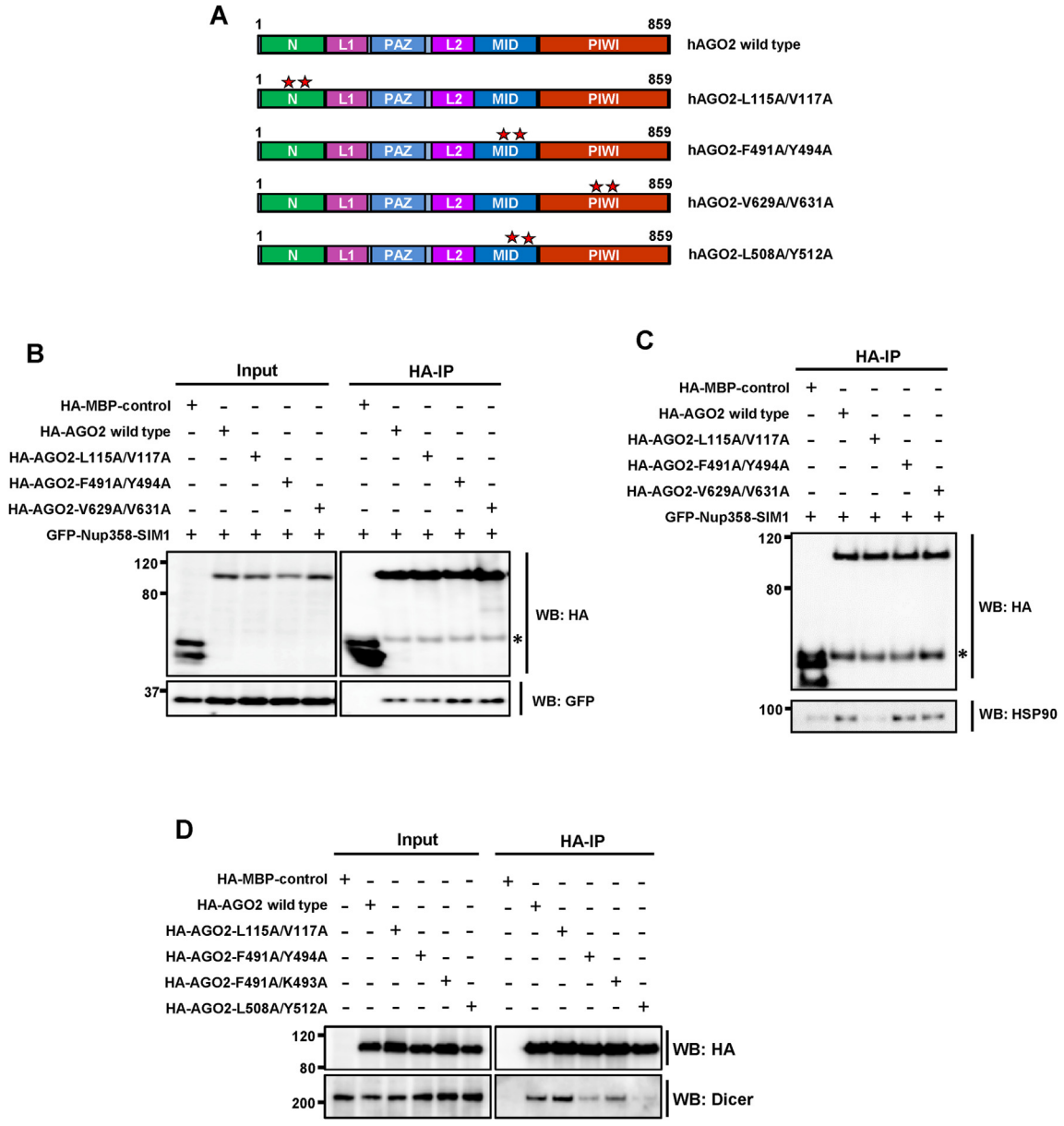

Fig. 1. Interaction of AGO2 mutants with Nup358-SIM1. (A) Schematic representation of hAGO2 double mutants analyzed in the study. (B) HEK293T cells were co-transfected with HA-MBP-control, HA-AGO2 wild type, or indicated AGO2 double mutants along with GFP-SIM1. HA immunoprecipitation (IP) was performed, followed by western blotting (WB) using indicated antibodies. (C) For interaction between HSP90 and different AGO2 mutants, the HA IP samples were probed with a specific antibody against HSP90. (D) HEK293T cells expressing indicated proteins were subjected to IP using HA antibody and endogenous Dicer in the immunoprecipitates were detected by Dicer-specific antibody. * indicates cross-reacting bands corresponding to IgG heavy chain.

300 s at the flow rate of 5 μl/min, and the dissociation was monitored for an additional 500 s. At the end of the complete binding cycle, regeneration was performed that removed the ligand and any bound analyte. Fresh Biotin CAPture Reagent was attached to the surface for each cycle. The SA CAP chip was regenerated by injecting 3 pulses of a regeneration solution made up of three parts of 8 M guanidine chloride (pH 8.0) and one part of 1 M NaOH for 15 s. The specific binding response was derived by subtracting the control flow cell data from the target protein immobilized flow cell data. The SPR data were evaluated using BIAevaluation software version 4.1 using global fitting (Biacore). The best-fitted model was selected by the software.

3. Results

3.1. Interaction of Nup358-SIM with AGO2 point mutants

Our previous studies indicated that Nup358-SIM, which interacts with SUMO, also binds AGO2. We reasoned that the region of SUMO that binds with SIM would have structural and sequence similarity with the region(s) in AGO2 that interacts with SIM. Therefore, to identify the possible sites on AGO2 involved in the interaction with Nup358-SIM (PDB ID: 1Z5S), we modeled AGO2-SIM interactions based on interface similarity. We detected regions on AGO2 (PDB ID: 4W5O) that were similar to the regions on SUMO that interacted with Nup358-SIM by CLICK [12,13], a

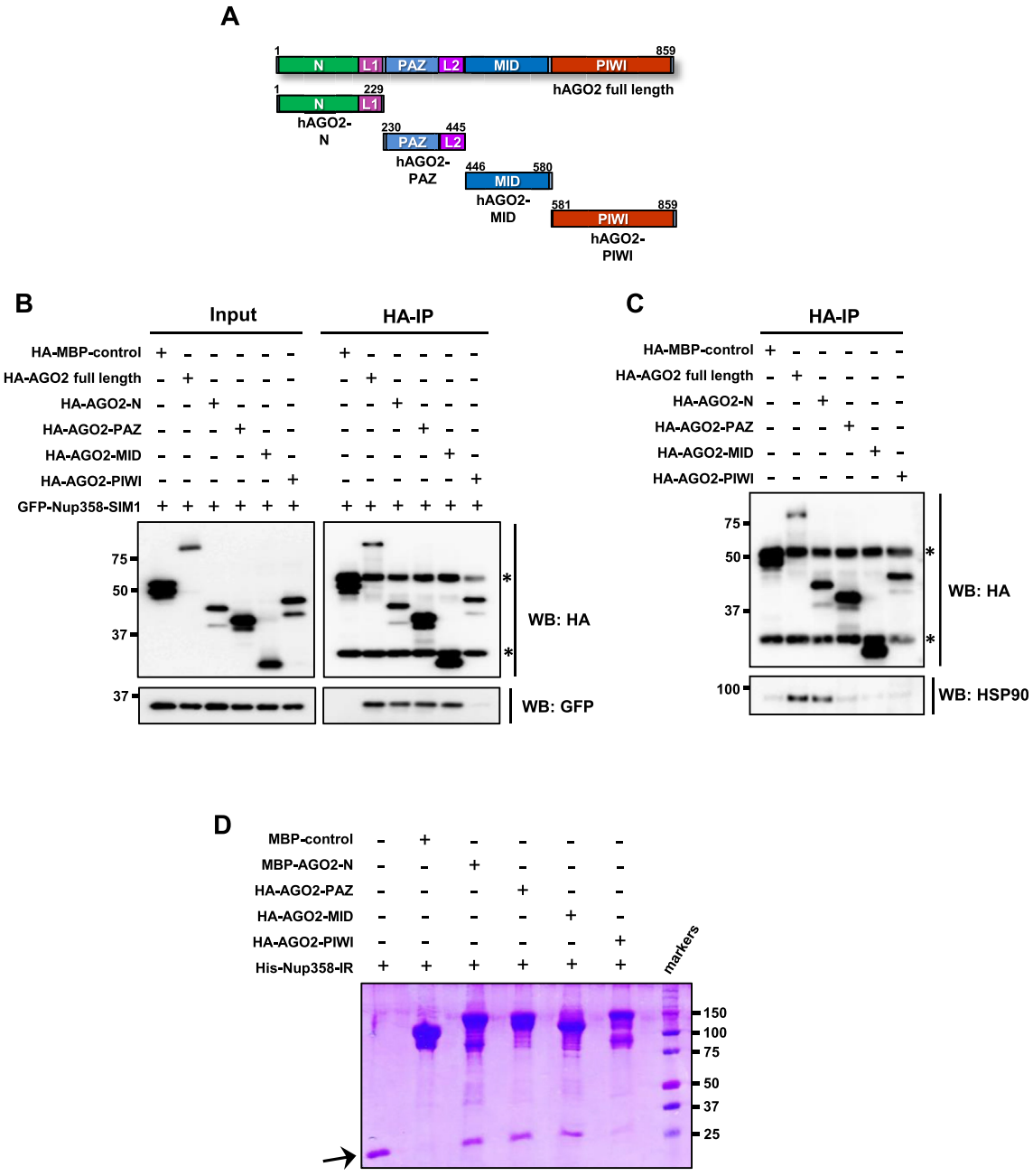

Fig. 2. N, PAZ and MID domains of AGO2 can independently interact with Nup358-SIM1. (A) Schematic representation of hAGO2 domains analyzed in the study. (B) HEK293T cells were co-transfected with HA-MBP-control, HA-AGO2 wild type or indicated fragments along with GFP-SIM1, and subjected to HA IP. The IP samples were analyzed by western blotting (WB) with indicated antibodies. (C) The HA IP samples were probed with a specific antibody to detect endogenous HSP90. * indicates cross-reacting bands corresponding to IgG heavy and light chains. (D) In vitro interaction studies using bacterially expressed proteins. MBP-control, MBP-AGO2-N, -PAZ - MID, or -PIWI domains were expressed in bacteria, purified with amylose beads and incubated with His-Nup358-IR1 (that contains two SIMs - SIM1 and SIM2). After the MBP-tagged proteins were pulled down, the presence of His-IR1 was detected by SDS-PAGE and coomassie staining. Arrow shows the band corresponding to His-Nup358-IR1.

program that recognizes structural similarity regardless of topology. The models were built using MODELLER [14], which predicted that Nup358-SIM would interact with three distinct domains of AGO2 - N, MID and PIWI - to be having regions structurally similar to SUMO1, which could thereby potentially bind to SIM [9].

To further characterize the interaction between Nup358 and AGO2 through SIM(s), point mutants of AGO2 through amino acid substitutions were generated based on the predictions using CLICK (Fig. 1A). Because of the expected similarity in the nature of interaction between SIM-SUMO and SIM-AGO2, the secondary structures and amino acids involved in the already known SIM-SUMO interaction interface were considered for the selection of residues in AGO2 for manipulation [10]. The mutations included L115A, V117A within the N domain; F491A, Y494A within the MID domain and V629A, V631A within the PIWI domain. These HA-AGO2 mutants were then tested for their ability to interact with GFP-tagged version of Nup358-SIM1 (GFP-SIM1) after co-expression in HEK293T cells, followed by co-immunoprecipitation assay (Fig. 1B). As expected, GFP-SIM1 was specifically co-immunoprecipitated with wild-type HA-AGO2 when compared to HA-MBP-control (Fig. 1B). Moreover, the different mutations designed to disrupt the interaction between AGO2 and SIM, based on the prediction

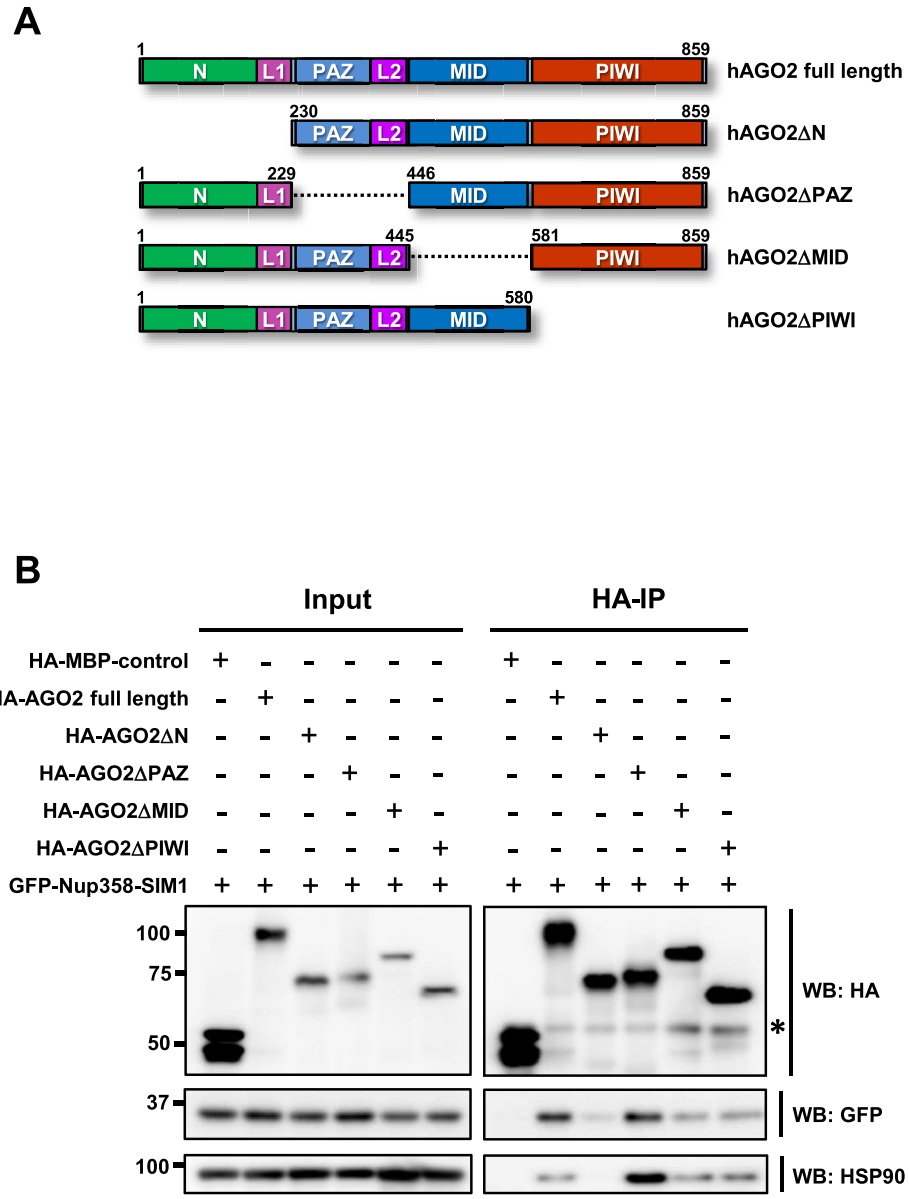

Fig. 3. N domain of AGO2 is important for its interaction with Nup358-SIM1. (A) Schematic representation of hAGO2 and deletion mutants analyzed in the study. (B) HEK293T cells were co-transfected with HA-MBP-control, HA-AGO2 wild type or indicated fragments along with GFP-SIM1, and subjected to HA IP. The IP samples were analyzed by blotting (WB) with indicated antibodies. Endogenous HSP90 in the IP samples was detected by HSP90-specific antibody. * indicates cross-reacting bands corresponding to IgG heavy chain.

using CLICK in the N, MID and PIWI domains of AGO2, did not affect their interaction significantly, indicating that these AGO2 residues may not contribute to the SIM interaction.

Although previous studies have shown the role of N and PIWI domains of AGO protein in the interaction with HSP90 and Dicer, respectively [7,8], the exact sites and residues within AGO involved in these interactions were not identified. We were interested in testing the ability of the generated AGO2 mutants in interaction with HSP90 and Dicer. Towards this, the HA-AGO2 wild-type and mutant immunoprecipitates were examined for the presence of endogenous HSP90 and Dicer. Interestingly, the interaction of HSP90 was significantly reduced in the case of L115A/V117A mutant as compared to wild-type AGO2 (Fig. 1C), indicating that the residues L115 and V117 are critically important for the binding of AGO2 with HSP90.

Results also suggested that F491 and Y494 within the MID domain are important for the interaction of AGO2 with Dicer. Another mutant, L508A/Y512A, also abrogated the interaction between AGO2 and Dicer (Fig. 1D), but not with SIM1 (Supplementary Table S1). Collectively, the results highlight the importance of AGO2 MID domain in general, and residues F491, Y494, L508 and Y512 within the MID domain, in mediating the interaction of AGO2 with Dicer.

3.2. Interaction of Nup358-SIM with AGO2 fragments

As mutations of none of the predicted residues in AGO2 resulted in compromised interaction with Nup358-SIM1, we resorted to a systematic analysis of individual domains of AGO2 (Fig. 2A) involved in the interaction with SIM. Different AGO2 domains were individually co-expressed with GFP-SIM1 in HEK293T cells and a co-immunoprecipitation assay was performed. The results showed that the AGO2 domains N, PAZ, MID, but not PIWI, interacted with SIM1 (Fig. 2B). Consistent with the earlier reports, HSP90

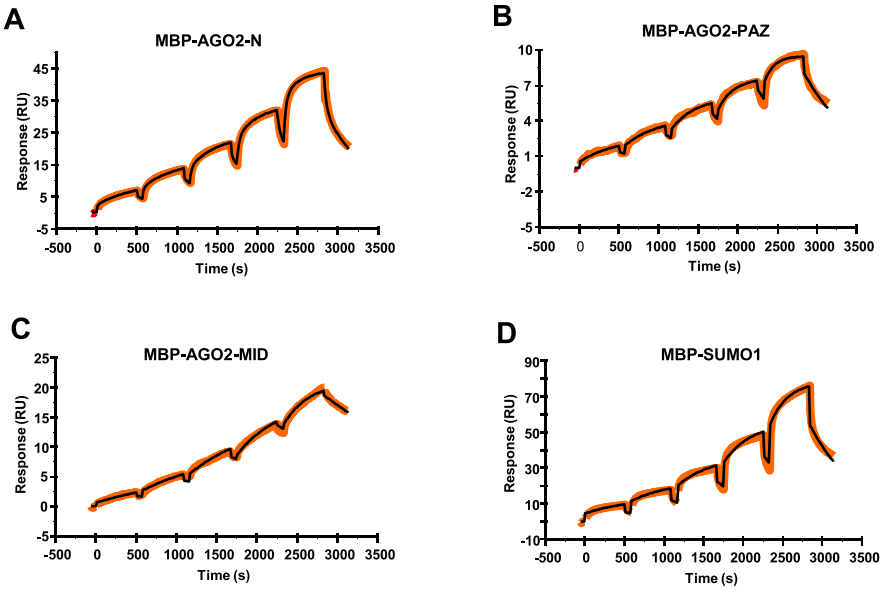

E

Analyte	kd1 ± SE	ka1 ± SE	KD1 (M)	kd2 ± SE	ka2 ± SE	KD2 (M)	Chi² (RU²)	Model used for data fitting
MBP-AGO2-N	$2.79x10^{-2}$ ± $2.23x10^{-4}$	3590 ± 15.34	$7.79x10^{-6}$	$9.62x10^{-4}$ ± $3.30x10^{-6}$	$8.85x10^{-5}$ ± $4.47x10^{-7}$	10.92	0.153	Bivalent
MBP-AGO2-N	$2.12x10^{-3}$ ± 7458	$4.5x10^{-6}$ ± 17	$2.85x10^{-7}$	–	–	–	0.472	Langmuir 1:1
MBP-AGO2-PAZ	$1.61x10^{-3}$ ± $5.53x10^{-6}$	8224 ± 23	$1.96x10^{-7}$	–	–	–	0.045	Langmuir 1:1
MBP-AGO2-MID	$5.63x10^{-4}$ ± $2.67x10^{-6}$	3307 ± 5.63	$1.7x10^{-7}$	–	–	–	0.071	Langmuir 1:1
MBP-SUMO1	$1.42x10^{-3}$ ± $5.67x10^{-6}$	2801 ± 12.67	$5.25x10^{-7}$	–	–	–	2.13	Langmuir 1:1

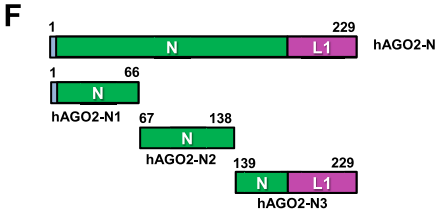

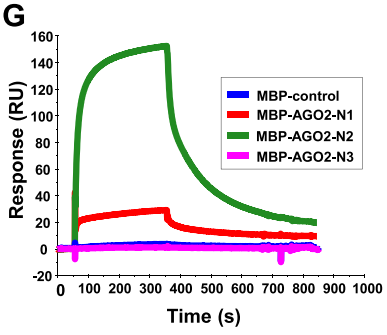

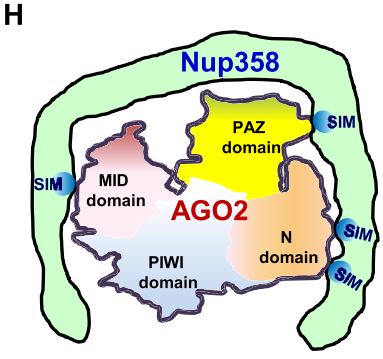

specifically interacted with the N domain of AGO2 (Fig. 2C).

Although our previous study had shown direct interaction between AGO2 and SIM [9], we wanted to test if SIM is directly bound to AGO2 N, PAZ, and MID domains. To explore this, in vitro pull-down assay using bacterially expressed MBP-tagged version of individual AGO2 domains and His-tagged Nup358-IR1 fragment that contains SIM1 was performed. The results showed that His-IR1 specifically co-purified with MBP-AGO2-N, -PAZ and -MID, as compared to AGO2-PIWI or MBP-control (Fig. 2D), demonstrating that SIM1 directly interacts with N, PAZ and MID domains.

3.3. Interaction of Nup358-SIM with AGO2 deletion mutants

To gain a better insight into the regions involved in AGO2 interaction with SIM, deletion mutants of AGO2 that lacked specific domains were used. Individual deletion mutant, HA-AGO2ΔN, HA-AGO2ΔPAZ, HA-AGO2ΔMID or HA-AGO2ΔPIWI (Fig. 3A), was co-transfected with GFP-SIM1 and their interaction was monitored by co-immunoprecipitation assay. Interestingly, as compared to full length or other AGO2 deletion mutants, the absence of N domain (AGO2ΔN) significantly reduced the interaction of AGO2 with GFP-SIM1 (Fig. 3B). These results indicated that although individually N, PAZ and MID can interact with Nup358-SIM (Fig. 2B,D), in the full-length context the interaction of SIM with the N domain of AGO2 appears to be critically important for the other domains (PAZ and MID) to bind to additional SIMs.

Consistent with previous studies [8] and our results in the current study (Figs. 1C and 2C) that HSP90 interacts with the N domain of AGO2, deletion of N domain, significantly reduced interaction of AGO2 with HSP90 (Fig. 3B).

3.4. SIM-AGO2 binding studies using surface plasmon resonance

To measure the affinities of AGO2 domains for SIM, surface plasmon resonance (SPR) was employed. Biotinylated SIM peptide (DNEIEVIIVWEKK) [11] was immobilized onto streptavidin chip, and purified individual domains of AGO2 or SUMO1 was used as analyte in the binding studies. The AGO2-N, -PAZ and -MID domains and positive control SUMO1 showed specific binding to SIM peptide (Fig. 4A–D). The results suggested that the apparent equilibrium dissociation constant (KD) for the interaction of SIM peptide with AGO2-N, -PAZ and –MID, when considered 1:1 binding model, was found to be comparable to that with SUMO1 (Fig. 4E). AGO2-N, -PAZ, -MID domains and SUMO1 interacted with SIM peptide with a dissociation constant of 285 nM, 196 nM, 170 nM and 524 nM, respectively. These results suggested that the binding affinity of SIM with individual AGO2 domains is more or less comparable to that with the known interactor SUMO1.

While the data for AGO2-PAZ, AGO2-MID and SUMO1 fitted well with 1:1 Langmuir binding model, the kinetic analysis using the best-fitting algorithm suggested AGO2-N to potentially contain two SIM-binding sites (Fig. 4E). We tested this possibility by using different regions within AGO2-N in the binding studies (Fig. 4F). The SPR analysis revealed that AGO2-N1 and -N2 specifically bound to immobilized SIM peptide, whereas AGO2-N3 and MBP-control showed no binding to SIM (Fig. 4G). Collectively, these data indicated that AGO2-PAZ and -MID domains have single binding sites for SIM1 as in the case of SUMO1, whereas AGO2-N has two probable binding sites, each one present within regions corresponding to 1–67 (N1) and 67–139 (N2) amino acid residues.

4. Discussion

Although it was shown that Nup358 interacts with AGO2 through SIMs, the nature of and regions in AGO2 involved in its interaction with Nup358 were unclear. In this study, our results suggest that Nup358 associates with AGO2 through multiple weak interactions mediated through SIMs. We also uncovered specific residues within the N domain and MID domain of AGO2 critical for interactions with HSP90 and Dicer, respectively.

Earlier molecular modeling studies predicted AGO2 to possess binding sites for Nup358-SIMs in the N, MID and PIWI domains [9]. Based on further analysis, we focused on specific residues in these regions that were mutated to Alanine to explore their contribution to the interaction with Nup358-SIM. However, mutations of none of the predicted residues, L115A/V117A within N domain, F491A/Y494 within MID-domain, or V629A/V631A within PIWI domain, compromised the interaction with SIM. It is well known that SIM-SUMO interaction majorly involves hydrophobic residues [15]. As all the predicted residues were substituted with Alanine, an amino acid with a hydrophobic side chain, our results do not completely rule out the possibility that they are not involved in the interaction with SIM. Future experiments with substitution of these and other potential residues with amino acids other than Alanine will help specify residues involved in AGO2-Nup358-SIM interactions.

In the current study, it was found that Nup358-SIM has multiple direct interaction sites within AGO2, specifically in the N, PAZ and MID domains. Even though these domains interacted with SIM independently, in the full-length context, the removal N domain led to a loss of AGO2-SIM interaction, indicating that the N domain is critical for this interaction. One possible explanation is that the N domain constitutes the primary binding site for SIM (or Nup358). This binding may exert conformational changes in the AGO2 molecule required for PAZ and MID to be accessible for interaction with other SIMs in Nup358. Nup358 possesses at least four SIMs (two verified and two predicted in the N-terminal, middle and C-terminal regions) and all the fragments containing these SIMs independently interact with AGO2 [9]. We do not know which SIM within Nup358 may bind to which domain within AGO2 protein to achieve the complex formation between these two proteins. However, structural and biochemical studies on the complex between Nup358 and AGO2 should shed light on these interactions in detail.

Based on the studies, a working model for intermolecular interaction between Nup358 and AGO2 is proposed (Fig. 4H). The present study suggests that Nup358-SIMs potentially make

Fig. 4. Surface plasmon resonance analysis of interaction between SIM peptide and AGO2 fragments. (A–D) Representative binding sensograms showing the interaction between the SIM peptide DNEIEVIIVWEKK and MBP-tagged version of AGO2 domains using single-cycle kinetics, and global fitting analysis was performed with multiple binding models (Biacore T200 Evaluation Software, version 3.1). MBP-SUMO1 was used as a positive control. The sensogram of SIM-AGO2-N interaction (A) fitted well with a bivalent analyte model, whereas SIM-AGO2-PAZ (B), SIM-AGO2-MID (C) and SUMO1 (D) fitted better with Langmuir 1:1 binding model. The real-time binding sensograms generated from this study are shown in red lines and the black lines represent the calculated global fitting model. (E) Kinetic data for the interactions of SIM peptide with AGO2-N, PAZ, MID and SUMO1. The level of biotinylated SIM1 peptide captured was 143 RU, 43 RU, 35 RU and 160 RU for MBP-AGO2-N, MBP-AGO2-PAZ, MBP-AGO2-MID and MBP-SUMO1, respectively. The data represented is the mean of three independent experiments. ka1, Association rate constant for the first site (M-1s-1); kd1, Dissociation rate constant for the first site (s-1); ka2, Association rate constant for the second site (RU-1s-1); kd2, Dissociation rate constant for the second site (s-1); KD1, Equilibrium dissociation constant for the first site (M); KD2, Equilibrium dissociation constant for the second site (M). SE, standard error. (F–G) Surface plasmon resonance (SPR) analysis for fragments within AGO2-N with SIM1. (F) Schematic representation of AGO2-N fragments (N1, N2 and N3) used in the study. (G) Binding kinetics of MBP-control, MBP-AGO2-N1, -N2 and N3 with SIM peptide. (H) Model depicting the possible interaction between Nup358 and AGO2 involving multiple Nup358-SIMs and regions of AGO2. (For interpretation of the references to colour in this figure legend, the reader is referred to the Web version of this article.)

multiple contacts within AGO2 through its N-, PAZ and MID-domains. Overall, it appears that the association of Nup358 with AGO2 might have regulatory functions. Nup358 may bind AGO2 through the multiple weak contacts to facilitate a stable association of miRNA-loaded AGO2 with the target mRNA.

In addition to providing insight into the molecular details of Nup358-AGO2 interactions, the current study also sheds light on specific AGO2 residues involved in the interaction with HSP90 and Dicer. Although previous reports have suggested HSP90 to interact with the N-terminal region of AGO2, and Dicer with the C-terminal half of AGO2 [6–8], specific residues involved in these interactions were not identified. Consistent with the earlier reports, co-immunoprecipitation assays showed that the N-domain fragment of AGO2 specifically interacted with HSP90, whereas AGO2ΔN mutant (N-domain deletion mutant) and AGO2-L115A-V117A mutants failed to interact with HSP90, indicating the critical requirement of these residues within the N-domain of AGO2 for interaction with HSP90. It was also found that mutations in the MID region (F491A/Y494A and L508A/Y512A double mutations) reduced the interaction of AGO2 with Dicer, suggesting a role for these specific AGO2 residues in binding to Dicer. Collectively, residues within AGO2 could be mapped, which are responsible for interaction with HSP90 and Dicer within N- and MID-domain, respectively.

Declaration of competing interest

The authors declare that they have no known competing financial interests or personal relationships that could have appeared to influence the work reported in this paper.

Acknowledgements

We thank H.N. Gopi, Indian Institute of Science Education and Research, Pune, for providing the peptides and Arvind Sahu, Janesh Kumar, Vasudevan Seshadri and their lab members (NCCS, Pune) for insightful discussions. We are grateful to Joseph lab members for the insightful discussions and suggestions. Timely help from Aparna Salunke (NCCS, Pune) is acknowledged. We also thank Mary Beulaa Jayaprakagasam (NCCS, Pune) for help with Biacore-SPR experiments. Financial support from Council of Scientific and Industrial Research, Government of India, to P.D. and from Department of Biotechnology, Government of India, to S.M., V.F. and Y.R is gratefully acknowledged. MSM acknowledges the DBT/Wellcome Trust India Alliance for a senior fellowship. The work was partly supported by intramural funding from NCCS and a grant (EMR/2014/001092) from Department of Science and Technology, Government of India.

Appendix A. Supplementary data

Supplementary data to this article can be found online at https://doi.org/10.1016/j.bbrc.2021.03.140.

References

[1] D.P. Bartel, MicroRNAs, Cell 116 (2004) 281–297.
[2] L.F.R. Gebert, I.J. MacRae, Regulation of microRNA function in animals, Nat. Rev. Mol. Cell Biol. 20 (2019) 21–37.
[3] G. Meister, Argonaute proteins: functional insights and emerging roles, Nat. Rev. Genet. 14 (2013) 447–459.
[4] M. Ha, V.N. Kim, Regulation of microRNA biogenesis, Nat. Rev. Mol. Cell Biol. 15 (2014) 509–524.
[5] J. Pfaff, G. Meister, Argonaute and GW182 proteins: an effective alliance in gene silencing, Biochem. Soc. Trans. 41 (2013) 855–860.
[6] H.-W. Wang, C. Noland, B. Siridechadilok, D.W. Taylor, E. Ma, K. Felderer, J.A. Doudna, E. Nogales, Structural insights into RNA processing by the human RISC-loading complex, Nat. Struct. Mol. Biol. 16 (2009) 1148–1153.
[7] N. Tahbaz, F.A. Kolb, H. Zhang, K. Jaronczyk, W. Filipowicz, T.C. Hobman, Characterization of the interactions between mammalian PAZ PIWI domain proteins and Dicer, EMBO Rep. 5 (2004) 189–194.
[8] N. Tahbaz, J.B. Carmichael, T.C. Hobman, GERp95 belongs to a family of signal-transducing proteins and requires Hsp90 activity for stability and golgi localization, J. Biol. Chem. 276 (2001) 43294–43299.
[9] M.R. Sahoo, S. Gaikwad, D. Khuperkar, M. Ashok, M. Helen, S.K. Yadav, A. Singh, I. Magre, P. Deshmukh, S. Dhanvijay, P.K. Sahoo, Y. Ramtirtha, M.S. Madhusudhan, P. Gayathri, V. Seshadri, J. Joseph, Nup358 binds to AGO proteins through its SUMO-interacting motifs and promotes the association of target mRNA with miRISC, EMBO Rep. 18 (2017) 241–263.
[10] O. Kerscher, SUMO junction—what's your function? EMBO Rep. 8 (2007) 550–555.
[11] A.T. Namanja, Y.-J. Li, Y. Su, S. Wong, J. Lu, L.T. Colson, C. Wu, S.S.C. Li, Y. Chen, Insights into high affinity small ubiquitin-like modifier (SUMO) recognition by SUMO-interacting motifs (SIMs) revealed by a combination of NMR and peptide array analysis, J. Biol. Chem. 287 (2012) 3231–3240.
[12] M.N. Nguyen, K.P. Tan, M.S. Madhusudhan, CLICK—topology-independent comparison of biomolecular 3D structures, Nucleic Acids Res. 39 (2011) W24–W28.
[13] M.N. Nguyen, M.S. Madhusudhan, Biological insights from topology independent comparison of protein 3D structures, Nucleic Acids Res. 39 (2011) e94.
[14] A. Šali, T.L. Blundell, Comparative protein modelling by satisfaction of spatial restraints, J. Mol. Biol. 234 (1993) 779–815.
[15] J.R. Gareau, C.D. Lima, The SUMO pathway: emerging mechanisms that shape specificity, conjugation and recognition, Nat. Rev. Mol. Cell Biol. 11 (2010) 861–871.